

MATHEMATICAL MODELING OF THE MOTION OF A LIQUID IN AN  
 AXISYMMETRIC TANK UNDER THE ACTION OF AN INJECTED JET

V. P. Koval' and A. V. Potapov

UDC 669.184:532.516

The velocity distribution is obtained for motion of a liquid in a tank under the action of a jet of gas injected through a free surface.

To calculate the melting of steel in a converter one must know the laws of heat and mass transfer in a pig-iron melt, acted on by a jet of oxygen. From the published papers one gets the impressions that it is impossible to describe the motion of the melt mathematically, and one must therefore use an experimental method of solution. Then a considerable amount of material must be expended to accomplish the technical proposals. However, the state of development of methods of solving the equations of liquid mechanics are such that a computer can be used to attempt a mathematical study of the converter hydrodynamics in order to seek scientifically based guidelines for improving the process.

Figure 1 shows a schematic of the converter. A jet of oxygen 3 is injected through the feed-line 2 into the melt 1 and forms a crater 4. Propagating along the surface of the crater, the jet interacts with the melt, creating forced motion in the tank.

Since the motion is axisymmetric, it is appropriate to seek a solution of the problem of the velocity distribution in the melt in terms of a cylindrical coordinate system  $r$ ,  $\varphi$ , and  $z$ . With continuous injection, the deviation of the melt velocity from a steady-state value can only occur because of variation of the melt density and viscosity with time. Taking the assumption that the melt motion is independent of time and this will be shown below, the initial dynamic equations for  $\partial/\partial t = \partial/\partial \varphi = 0$  can be written in the form

$$\begin{aligned} v_r \frac{\partial v_r}{\partial r} + v_z \frac{\partial v_r}{\partial z} &= F_r - \frac{1}{\rho} \frac{\partial P}{\partial r} + v_T \left( \frac{\partial^2 v_r}{\partial r^2} + \frac{1}{r} \frac{\partial v_r}{\partial r} - \frac{v_r}{r^2} + \frac{\partial^2 v_r}{\partial z^2} \right), \\ v_r \frac{\partial v_z}{\partial r} + v_z \frac{\partial v_z}{\partial z} &= F_z - \frac{1}{\rho} \frac{\partial P}{\partial z} + v_T \left( \frac{\partial^2 v_z}{\partial r^2} + \frac{1}{r} \frac{\partial v_z}{\partial r} + \frac{\partial^2 v_z}{\partial z^2} \right), \\ \frac{\partial (rv_r)}{\partial r} + \frac{\partial (rv_z)}{\partial z} &= 0. \end{aligned} \quad (1)$$

In deriving the system of equations (1) we assumed that the turbulent analog of the viscosity  $v_T$  is independent of coordinates  $r$  and  $z$ , and we could then take it outside the differentiation sign. For large Reynolds numbers this assumption is based on the Kolmogorov turbulence model [1]. To use a representation of  $v_T$ , based on the well-known semiempirical theories, would lead to a complication in Eq. (1), leaving us with the same hypothesis. After reducing the equations to dimensionless form, we introduce  $v_T$  into the turbulent analog of the Reynolds number  $Re_T$ , based on a semiempirical formula relating it to the tank dimensions, the injection conditions, and the physical properties of the liquid.

To solve the system of equations we must know the velocity distribution along the tank axis, on the bottom, the walls, and the free surface of the liquid. From the flow symmetry condition, along the tank axis we have

$$v_r = 0, \quad \frac{\partial v_z}{\partial r} = 0. \quad (2)$$

Dnepropetrovsk State University. Translated from *Inzhenerno-Fizicheskii Zhurnal*, Vol. 32, No. 3, pp. 443-448, March, 1977. Original article submitted March 30, 1976.

*This material is protected by copyright registered in the name of Plenum Publishing Corporation, 227 West 17th Street, New York, N.Y. 10011. No part of this publication may be reproduced, stored in a retrieval system, or transmitted, in any form or by any means, electronic, mechanical, photocopying, microfilming, recording or otherwise, without written permission of the publisher. A copy of this article is available from the publisher for \$7.50.*

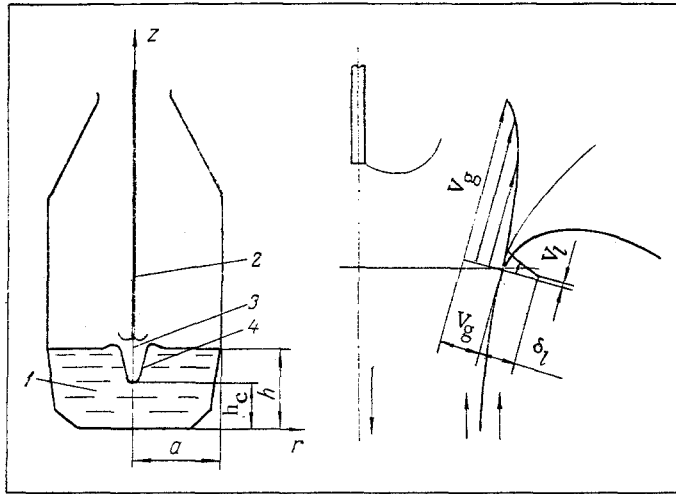


Fig. 1. Schematic of the converter.

On the bottom and the walls, using the conditions of impermeability and zero slip of the liquid, we have

$$v_r = 0, \quad v_z = 0. \quad (3)$$

To define the boundary condition on the free surface we use an approximate velocity distribution obtained from physical reasoning and including a conceptual interaction of the gas jet with the liquid.

To estimate the order of magnitude of the velocity and choose a characteristic value  $V = \sqrt{V_r^2 + V_z^2}$ , we examine the gas motion along the liquid surface. From the condition that the tangential stresses are equal on the crater surface

$$\left( \mu \frac{\partial v}{\partial n} \right)_g = \left( \mu \frac{\partial v}{\partial n} \right)_l,$$

assuming a linear velocity distribution in the boundary layers, and taking into account that  $V_l \ll V_g$ ,  $\mu_g \ll \mu_l$ , we obtain the following relation for the velocity of the interface:

$$V \sim \left( V \frac{\mu}{\delta} \right)_g \left( \frac{\delta}{\mu} \right)_l,$$

where  $\mu$ ,  $\delta$  are the dynamic viscosity and the boundary layer thickness, respectively.

In [2], in an experimental study of the motion of a swirling jet of air above a water surface, the authors obtained  $V_g/V_l = 55$ , which corresponds to the value calculated from the viscosity ratio. For interaction of oxygen, heated to 500°C, with a pig-iron melt,  $V_g/V_l \approx 50$ , and the maximum velocity of the crater surface is 3-4 m/sec. We define the crater diameter and depth from the known empirical relations [3]. Taking the above into account, the velocity distribution in the crater zone can be described by the linear relations

$$\begin{aligned} v_z &= \frac{r}{kr_c} V_z \text{ for } 0 < r < kr_c; \\ v_z &= \frac{r_c - r}{(1-k)r_c} V_z \text{ for } kr_c < r < r_c; \\ v_r &= V_r \frac{h_c - z}{h_c - h} \text{ for } h_c < z < h, \end{aligned} \quad (4)$$

where  $kr_c$  is the crater radius corresponding to velocity  $V$ .

We now convert the system of equations (1) to a form suitable for numerical solution. We introduce the stream function  $\psi$ , the vorticity  $\omega$ ,

$$v_r = \frac{1}{r} \frac{\partial \psi}{\partial z}, \quad v_z = -\frac{1}{r} \frac{\partial \psi}{\partial r}, \quad \omega = \frac{\partial v_r}{\partial z} - \frac{\partial v_z}{\partial r}, \quad (5)$$

and the dimensionless quantities

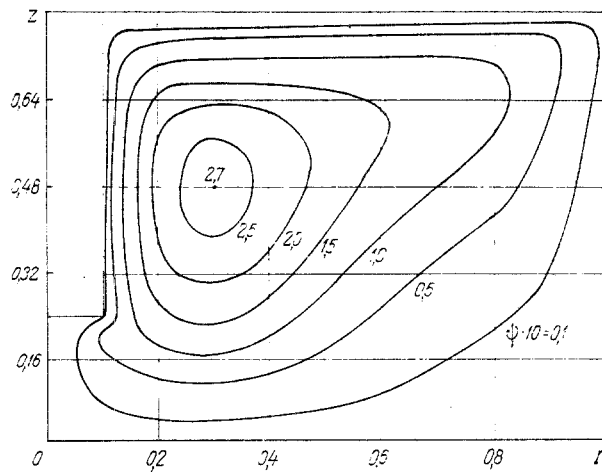


Fig. 2. Distribution of the stream function in the meridional plane.

$$\bar{r} = \frac{r}{a}, \quad \bar{z} = \frac{z}{a}, \quad \bar{\psi} = \frac{\psi}{Va^2}, \quad \bar{\omega} = \frac{\omega a}{V}, \quad Re_T = \frac{Va}{\nu_T}, \quad (6)$$

where we drop the bars above the symbols for simplicity. We eliminate the pressure  $P$  and the mass force components from the system (1). To do this we differentiate the first equation with respect to  $z$ , the second to  $r$ , and subtract one from the other. After reducing this equation and Eq. (5) to dimensionless form, and taking account of Eq. (6), we obtain

$$r^2 \left[ \frac{\partial}{\partial z} \left( \frac{\omega}{r} \right) \frac{\partial \psi}{\partial r} - \frac{\partial}{\partial r} \left( \frac{\omega}{r} \right) \frac{\partial \psi}{\partial z} \right] + \frac{1}{Re_T} \left\{ \frac{\partial}{\partial z} \left[ r^3 \frac{\partial}{\partial z} \left( \frac{\omega}{r} \right) \right] + \frac{\partial}{\partial r} \left[ r^3 \frac{\partial}{\partial r} \left( \frac{\omega}{r} \right) \right] \right\} = 0, \quad (7)$$

$$\frac{\partial}{\partial z} \left( \frac{1}{r} \frac{\partial \psi}{\partial z} \right) + \frac{\partial}{\partial r} \left( \frac{1}{r} \frac{\partial \psi}{\partial r} \right) = \omega.$$

As unknowns in the equations we introduce the stream function  $\psi$  and the vorticity  $\omega$ , functions of the coordinates  $r$  and  $z$ . We define the turbulent analog of the Reynolds number  $Re_T$  from the semiempirical relation

$$Re_T = \lg \left[ Re \left( \frac{d_c \delta}{a^2} \right)^2 \right], \quad (8)$$

where

$$Re = \frac{U \cdot 2a}{\nu}$$

and the liquid velocity, averaged over the boundary-layer thickness for a characteristic crater section, is

$$U = \frac{1}{\delta} \int_0^{\delta} v dn.$$

In order to represent a change of viscosity and melt density, typical for the melting of steel in an oxygen converter [4], the value of  $Re_T$  remains practically constant during the gas injection. The mixing can be intensified by increasing  $Re_T$  until one reaches a similarity regime with a corresponding structure of turbulence, and by changing the velocity  $U$ , one can proceed until the crater surface becomes unstable, when the converter output increases sharply.

The region of solutions of Eq. (7) is shown in Fig. 2. The crater profile is approximated by a rectangle of sides  $h_c \times r_c$ . In the solution we used the uniform mesh

$$z_i = i \cdot \Delta z, \quad \Delta z = \frac{h}{m}, \quad i = 0, 1, \dots, m;$$

$$r_j = j \cdot \Delta r, \quad \Delta r = \frac{1}{n}, \quad j = 0, 1, \dots, n.$$

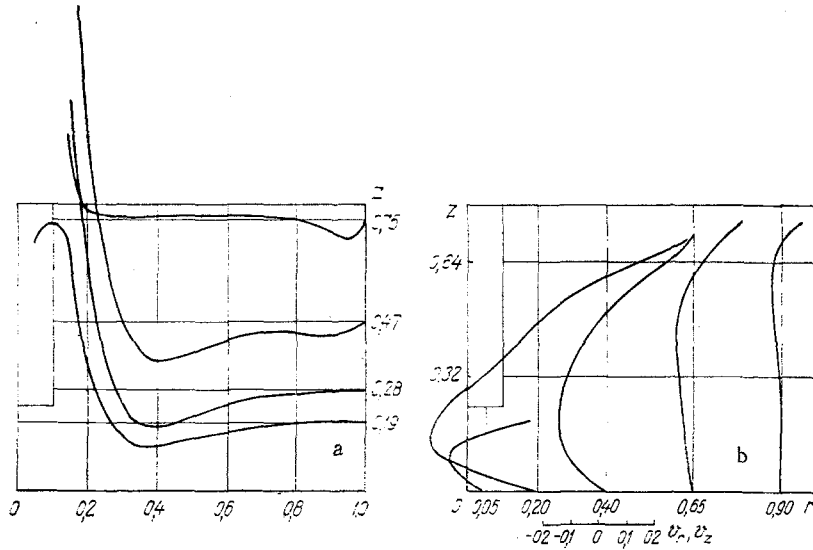


Fig. 3. Velocity distribution in the meridian plane:  
a) axial; b) radial.

The boundary conditions for the vorticity were obtained in dimensionless form from Eqs. (2)-(4), taking account of Eq. (5):

on the tank axis with  $r = 0$ ,  $0 < z < h_c$ ,  $i = 0, 1, \dots, i1$

$$\omega_{i,0} = 0; \quad (9)$$

in the crater with  $0 < r < r_c$ ,  $z = h_c$ ,  $j = 0, 1, \dots, j1$

$$\omega_{i1,j} + \frac{\omega_{i1-1,j}}{2} = \frac{3}{r_{i1,j}} \frac{\psi_{i1-1,j} - \psi_{i1,j}}{(\Delta z)^2} - \frac{3}{2} \left( \frac{\partial v_z}{\partial r} \right)_{i1,j}; \quad (10)$$

for  $r = r_c$ ,  $h_c < z < h$ ,  $i = i1, \dots, m$

$$\left( 1 + \frac{\Delta r}{r_c} \right) \omega_{i,j1} + \frac{\omega_{i,j1+1}}{2} = \frac{3}{r_c} \frac{\psi_{i,j1+1} - \psi_{i,j1}}{(\Delta r)^2} + 3 \left( 0.5 + \frac{\Delta r}{3r_c} \right) \left( \frac{\partial v_r}{\partial z} \right)_{i,j1}; \quad (11)$$

on the free surface with  $r_c < r < 1$ ,  $z = h$  ( $j = j1, \dots, n$ )

$$\omega_{m,j} + \frac{\omega_{m-1,j}}{2} = \frac{3}{r_{m,i}} \frac{\psi_{m-1,j} - \psi_{m,j}}{(\Delta z)^2} + V_r \frac{3}{\Delta z}; \quad (12)$$

on the side wall with  $r = 1$ ,  $0 < z < h$  ( $i = 0, 1, \dots, m$ )

$$(1 + \Delta r) \omega_{i,n} + \frac{\omega_{i,n-1}}{2} = 3 \frac{\psi_{i,n-1} - \psi_{i,n}}{(\Delta r)^2}; \quad (13)$$

on the tank bottom with  $0 < r < 1$ ,  $z = 0$  ( $j = 0, 1, \dots, n$ )

$$\omega_{0,j} + \frac{\omega_{1,j}}{2} = \frac{3}{r_{0,j}} \frac{\psi_{1,j} - \psi_{0,i}}{(\Delta z)^2}. \quad (14)$$

The stream function along the contour of the region examined is

$$\psi = 0. \quad (15)$$

This system of equations (7), of elliptic type with boundary conditions (9)-(15), was solved by a mesh method, using a Zeidel iteration scheme on a type M-222 computer.

By way of example we calculated the velocity field in the tank of a 130-ton converter with dimensions  $a = 2$  m,  $h/a = 0.8$ ; for crater dimensions  $2r_c = 0.4$  m,  $r_c/h_c = 0.38$ . The kinematic viscosity of steel was assumed to be  $\nu = 0.8 \cdot 10^{-6}$  m<sup>2</sup>/sec for 1600°C. With a characteristic velocity of the crater surface of  $V = 4$  m/sec,  $U \approx 0.5 V$  and a boundary-layer thickness of  $\delta = 0.02$  m,  $Re_T = 1$ . It can be seen from Fig. 2 that the injected jet forms a toroidal vortex in the melt, with motion toward the bottom of the tank near the walls, and toward the free surface in the axial zone. The maximum values of axial velocity are at the level of the vortex center, and the maximum radial velocity is on the free surface and below

the crater (Fig. 3). Near the walls and on the tank bottom the velocity components are small, with a strong attenuation from the free surface to the bottom.

The results of the calculations show that the velocity distribution agrees with the experimental data [3].

#### NOTATION

$\alpha$ , tank radius;  $h$ , tank height, crater depth;  $F$ , mass force;  $v, V$ , velocities;  $P$ , pressure;  $Re_T$ , turbulent analog of the Reynolds number;  $r, z$ , coordinates;  $\delta$ , boundary-layer thickness;  $\rho$ , density;  $\nu_T$ , turbulent analog of the viscosity;  $\psi$ , stream function;  $\omega$ , vorticity. Indices:  $g$ , gas;  $l$ , liquid;  $c$ , crater;  $(i, j)$ , node of the rectangular mesh;  $il$ , node corresponding to  $h_c$ ;  $jl$ , node corresponding to  $r_c$ .

#### LITERATURE CITED

1. A. N. Kolmogorov, Dokl. Akad. Nauk SSSR, 30, No. 4 (1941).
2. A. V. Tonkonogii, A. V. Ul'yanov, and D. B. Kozhakhmetov, in: Problems in Heat Engineering and Applied Thermophysics [in Russian], No. 2, Izd. Nauka Kazakh SSR, Alma-Ata (1965).
3. V. I. Yavoiskii, G. A. Dorofeev, and I. L. Povkh, Theory of Cooling of Steel Melt Tanks [in Russian], Metallurgiya, Moscow (1974).
4. J. F. Elliot et al., Thermochemistry for Steelmaking, Addison-Wesley (1960).

#### INFLUENCE OF THE PROPERTIES OF HYDRATED SOLID PHASE SURFACES ON THE EFFECT OF A DENSITY CHANGE IN A DISPERSED MEDIUM

P. P. Olodovskii

UDC 541.18.051

The role of exchange cations in the formation of the structure of a dispersed medium on hydrated surfaces of montmorillonite is shown.

Results of experimental investigations associated with the proof of the existence of an effect of a density change in a dispersed medium in a solid-adsorbed water-liquid system and an interpretation of these results on the basis of a mechanism of adsorption of the dispersed medium molecules on active centers of clayey mineral surfaces are presented in [1].

Taking account of this effect permitted a more confident estimation of the density distribution of the adsorbed water and giving a foundation to methods of computing the adsorption characteristics of dispersed systems. But it is interesting to extend the investigation and to establish the influence of the active center configuration in the solid phase on both the change in structure of the dispersed medium on the boundary with this phase and on the density of the adsorbed water.

The natural form of montmorillonite (Crimean kill) was taken as the subject of the study, it being selected also because it was necessary to establish the role of the specific surface of different sections of the crystal lattice in the formation of the filtration properties of a mineral modified by water-soluble polymers.

The first step in the research was to determine the density of the dehydrated adsorbent  $d_0$  in a fluid possessing a zero effect of a change in its density, i.e., the density of the solid phase in such a fluid is independent of its mass. As for Na-montmorillonite, nitrobenzene is a fluid with zero effect for the natural form of bentonite. According to the

---

Central Scientific-Research Institute of the Complex Utilization of Water Resources, Ministry of Water Resources of the USSR, Minsk. Translated from Inzhenerno-Fizicheskii Zhurnal, Vol. 32, No. 3, pp. 449-457, March, 1977. Original article submitted February 6, 1976.

*This material is protected by copyright registered in the name of Plenum Publishing Corporation, 227 West 17th Street, New York, N.Y. 10011. No part of this publication may be reproduced, stored in a retrieval system, or transmitted, in any form or by any means, electronic, mechanical, photocopying, microfilming, recording or otherwise, without written permission of the publisher. A copy of this article is available from the publisher for \$7.50.*